**Known instrumental effects that affect the OML1B product of the Ozone Monitoring Instrument on EOS Aura**

Marcel Dobber
Last update 7 June 2006.

***References:***

RD01 GDPS Input / Output Data Specification (IODS) Volume 2: Level 1B output products and metadata, SD-OMIE-7200-DS-467, issue 3, 24 February 2005.
RD02 G. H. J. van den Oord, J. P. Veefkind, P. F. Levelt, M. R. Dobber, Level 0 to 1B processing and operational aspects, IEEE Trans. Geosc. Rem. Sens. **44** (5), pp 1380-1397 (2006).
RD03 GDPS Input / Output Data Specification (IODS) Volume 4: Operational Parameters File Specification , SD-OMIE-7200-DS-488, issue 4, 28 March 2005.
RD04 Transient signal flagging algorithm definition for radiance data, TN-OMIE-KNMI-717, issue 2, 12 July 2005.
RD05 Transient signal flagging algorithm definition for non-radiance data, TN-OMIE-KNMI-718, issue 2, 12 July 2005.
RD06 OMI GDPS algorithm to correct for wavelength shifts due to inhomogeneous slit illumination, TN-OMIE-KNMI-680, issue 1, 17 January 2005.
RD07 In-flight wavelength assignment: correcting for inhomogeneous slit illumination, TN-OMIE-KNMI-692, issue 1, 17 March 2005.
RD08 Reducing along-track stripes in OMI-Level 2 products, TN-OMIE-KNMI-785, version 1.0, 13 March 2006.
RD09 Ozone Monitoring Instrument calibration, M. R. Dobber, R. J. Dirksen, P. F. Levelt, G. H. J. van den Oord, R. Voors, Q. Kleipool, G. Jaross, M. Kowalewski, E. Hilsenrath, G. Leppelmeier, J. de Vries, W. Dierssen, N. Rozemeijer, IEEE Trans. Geosc. Rem. Sens. **44** (5), pp 1209-1238 (2006).

**General**

The detailed GDPS operational 0-1 processor details are not discussed here, the reader is referred to RD01-RD03. The level-1b output products and metadata is described in detail in RD01. More details on the OMI instrument design characteristics and on the on-ground and in-flight calibration details are given in RD09.

General-1)
Proton radiation damage: Background correction.
Proton-induced radiation damage on the CCD detectors leads to the following effects observed in unbinned pixels:
1) Increase in dark current by a factor of at least 4-5.
2) RTS behaviour (see below) after the pixel has been hit.

The effects in the unbinned pixels obviously also transfer into the behaviour of the binned pixels than contain the unbinned pixels that were hit by protons. The rate at which pixels are hit in the UV and VIS channels (image and storage sections of the CCD detectors) is about 29 unbinned pixels per day per detector per region. The damage occurs mostly via trapped protons in the South-Atlantic Anomaly (SAA) and in the radiation belts close to the north and south poles. The aluminium shielding with an average thickness of about 29 mm is not capable of stopping high-energetic protons (e.g. >100 MeV) before they reach the CCD detectors. In addition, high-energetic protons may create secondaries in the aluminium shielding, which in turn may yield additional damage to the CCD detectors.
Both effects require frequent updates of the background images contained in the OPF for the background subtraction algorithm in the 0-1 data processor. Currently these background images are updated only once per month and just after updating the background images the time difference between the measurements and the measurement time of the background images is typically about five days. This results in sub-optimal background subtraction for pixels that are hit

after the OPF has been updated. The resulting effect is spikes in the background corrected images. In the future background images will be used from the same day as the light measurements. This can only be done when the time-dependent OPF system will have become operational.

General-2)
Proton radiation damage: Random Telegraph Signals (RTS)
See also above (proton radiation damage: background correction).
After a pixel has been hit by a proton it develops RTS, i.e. the response of the pixel without illumination jumps in time between at least two signal levels. Of course this also occurs in case of illumination. The time periods between the jumps can be from seconds to even days. The amplitude between the jumps can also vary greatly between the original dark current and about 4-5 times the original dark current. The different signal levels can be more or less stable, or show exponential decrease or increase with time. It can not be predicted what behaviour a pixel will show when it is hit. It is only possible before the pixel is hit to express statistically what the chance is that a pixel will show certain behaviour. Once a pixel has in fact been hit, it is possible to express statistically what the chance is that it will be at a certain signal level. It is not possible to predict with 100% certainty what the signal level of that specific pixel will be. The RTS behaviour makes the background correction algorithm less accurate. Even with the most recent background images in the OPF, it is not possible to correct for the background signal of RTS pixels with the same accuracy as for pixels that do not show RTS, because as a result of the statistical nature of the RTS it is not possible to predict the signal level of such a pixel beforehand. When the RTS is too severe, the pixel may become practically unusable. As a rough rule we estimate that this is the case for about 5% of the unbinned pixels that have been hit by a proton. As an indicator, this would be about 145 pixels in 100 days. The total amount of pixels is 780x576=449280, so roughly 0.03% of the pixels becomes unusable per 100 days per detector per region. The number of 5% is somewhat arbitrary and is likely to be different for different level-2 data products (higher for level-2 data products that depend more critically on the accuracy of the background correction).
It must be realised that these numbers apply to the unbinned case. When one unbinned pixel shows severe RTS, binned pixels may also become unusable. For global measurements (binning factor 8) the number of 0.03% per 100 days unbinned pixels corresponds to about 0.3% per 100 days for pixels with binning factor 8.
(Binned) pixels that show too severe RTS have been flagged in the level-1 data by the 0-1 data processor by using an unbinned map to identify severe RTS pixels. These flags have been set conservatively in order to avoid flagging a large percentage of the data. However, it is advised to exclude flagged RTS pixels from subsequent data analysis.

General-3)
Proton radiation damage: Transients.
See also above (proton radiation damage: background correction).
Pixels that are hit by protons or other particles can show subsequent permanent or longer lasting damage effects. However, it is also possible that pixels are hit and only show significantly increased signal during one readout, a so-called transient spike. In the readouts following the one in which the hit occurred no lasting effects of the hit can be found. In the GDPS dedicated algorithms have been developed for radiance and irradiance measurement data in order to identify and flag these transient spikes (RD04 and RD05). In case a transient is detected the pixel quality flag (bit number 3) for that detector pixel is raised. In certain regions on the earth the number of transient spikes is higher than in the remaining regions, e.g. in the radiation belts close to the north and south poles and in the south Atlantic anomaly.

General-4)
Stripes (variability with viewing angle) in various level 2 data products originating from level 1 radiance and irradiance data.
Several level 2 data products show features as a function of swath angle, so-called stripes. These features can persist over an entire orbit or even over more orbits. An example is shown in figure 1

below. Although the stripes in the level 2 data products must originate from swath-angle-dependent features in the level 1 data, they are not easily visible in the level 1 data.

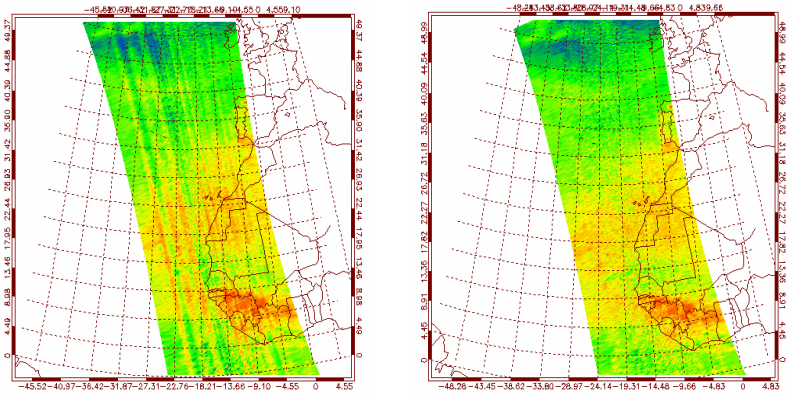

Figure 1: Nitrogen dioxide level 2 data product result for a specific orbit over west Africa. The left figure shows the along-track stripes at certain cross-track swath viewing angles. The right figure shows the same orbit with reduced stripes.

The stripe phenomenon was carefully investigated by investigating the impact on the nitrogen dioxide retrieval in the visible channel. The results are given in RD08. It was shown that the amplitudes of the stripes can be reduced by a factor of 3-4 when images from the same orbit are used for the background correction of the light images. This is currently not possible, but in the future use of background image correction using background images from the same day will be implemented when the time-dependent OPF will have become operational.
The persisting stripes over an orbit originate from the irradiance product used to calculate the earth reflectance (ratio earth radiance / sun irradiance) for the orbit under investigation. These stripes can be further reduced by using dedicated and specially constructed solar irradiance products. The solar irradiance product needs to be optimised separately for different wavelength ranges and different level 2 data products. However, since the construction of these dedicated products can only be obtained by combining level 1 data and level 2 data, it was decided not to pursue this path further in the operational data processing chains.
In summary, the current level 1 data products contain features that can lead to stripes in the level 2 data products. This will be improved in the future by using daily background maps when the time-dependent OPF will be operational. Then, the remaining stripes in the nitrogen dioxide level 2 product are comparable to the noise level of the OMI instrument.

General-5)
Gain switching columns.
The CCD can have in the column (wavelength) dimension up to four regions with different electronic gain settings. These regions are separated by up to three gain switching column, that can be located in columns in the full-performance range of the instrument. During on-ground testing it has been observed that 2-3 columns higher than the gain switching columns show electronic settling effects. These effects are corrected for in the GDPS, but the result after correction may still be less accurate than columns located more than three columns higher than the gain switching columns.

General-6)
Pixel-to-pixel Response Non-Uniformity (PRNU).
The CCD detectors show pixel-to-pixel response non-uniformity variations of up to 5%. These variations are more or less diagonal over the CCD detectors and are most pronounced in the ultraviolet wavelength range (up to 5%) and far less pronounced in the visible wavelength range (< 0.1%). The effect is corrected for in the 0-1 data processing, but the correction is not perfect. Residual errors of up to 0.1-0.2% may be observed in some cases in the individual radiance or

irradiance spectra. The PRNU effect or residual errors cancel to a large degree when the ratio of radiance over irradiance data is calculated.

General-7)
Entrance slit irregularities.
The entrance slit of the OMI spectrometer has a nominal width of 300 μm and a length of about 40 mm and is known to show width variation along the length of the slit of up to several percent. The effect is sufficiently wavelength independent, but manifests itself differently in the UV1, UV2 and VIS optical subchannels. The effect is corrected for in the 0-1 data processing, but the correction is not perfect. Residual errors of up to 0.1-0.2% may be observed in some cases in the individual radiance or irradiance spectra. The slit irregularity effect or residual errors cancel to a large degree when the ratio of radiance over irradiance data is calculated.

**Level 1 irradiance data**

Irradiance-1)
Spectral stray light correction.
The spectral stray light correction algorithm that is currently implemented in the 0-1 data processor calculates the source contributions by using measurement data from all viewing directions (rows) and applies the correction to the target region with the same magnitude and wavelength dependence for all rows. This approach was originally chosen to avoid introducing additional measurement noise with the spectral stray light correction algorithm. However, this approach yields sub-optimal results in case of inhomogeneous illumination conditions over the CCD rows (viewing directions). Viewing directions (rows) with low signals are over-corrected and viewing directions with high signals are under-corrected. For radiance data the viewed ground scenes are far more inhomogeneous than for the viewed scenes of the irradiance data. For the irradiance the errors are estimated to be below 0.5% as a result of the homogeneous illumination conditions.

Irradiance-2)
Irradiance goniometry correction.
The irradiance calibration depends on the azimuth (seasonal dependence) and elevation (orbital position dependence) angles, as well as on the viewing angle (row), wavelength (column) and on-board diffuser employed for the solar measurement. The currently implemented calibration keydata in the OPF for the quartz volume diffuser and the algorithm in the 0-1 data processor for the irradiance goniometry correction are not perfect. Row dependent errors of up to 0.5% in UV1 and UV2 and up to 0.2% in VIS can remain after correction.

Irradiance-3)
Diffuser spectral and spatial features.
It has been known already since the on-ground performance verification and calibration that the on-board diffusers show spatial (row-dependent) and spectral (column dependent) features that change with azimuth and elevation angles of incidence on the diffuser surface. The spatial features have amplitudes of up to 4% for the aluminium diffusers and 0.1% for the quartz volume diffuser. The spectral features have periods of typically 5-10 nm and amplitudes of up to typically 4% for the aluminium diffusers and 0.1% for the quartz volume diffuser. The quartz volume diffuser is used for the daily solar measurements that are processed by the 0-1 data processor into the official level-1b irradiance product. The solar measurements via the aluminium diffusers are performed once per week (regular aluminium diffuser) and once per month (backup aluminium diffuser). These measurements via the aluminium diffusers are stored only in the level-1b calibration files.

Irradiance-4)
Irradiance absolute radiometric calibration.
UV2-VIS.

The irradiance absolute radiometric calibration has been calibrated by comparing the measured irradiance with a high-resolution solar reference spectrum convolved with the OMI spectral slit functions, that have been accurately calibrated on the ground. Any deviations from one in the ratio of these two spectra can result from inaccuracies in:

- The spectral assignment in the measured irradiance.
- The spectral slit functions.
- The high-resolution solar reference spectrum.
- The irradiance absolute radiometric calibration.

The current result is shown in figure 2.

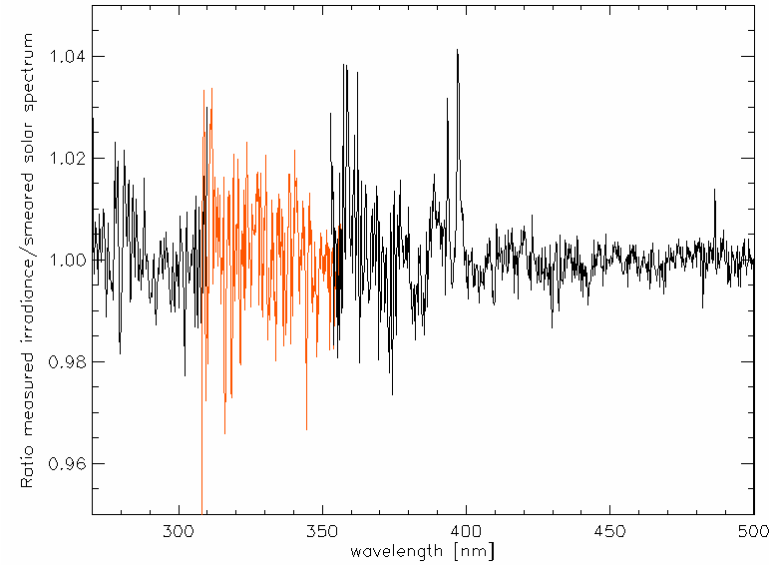


Figure 2: Ratio measured irradiance / high-resolution solar spectrum convolved with spectral slit functions for orbit 2465 (31 December 2004).

Some residual structure in the order of 1-2% remains. The CaII lines show up with an amplitude of about 3-4%, which can be tentatively attributed to differences in the high-resolution solar reference spectrum with regards to solar activity.
However, if changes are made to GDPS algorithms that are applied in the processing chain prior to the radiometric calibration, changes will also occur to the final results and the result as shown in figure 2. For example, if the stray light algorithm that uses the lower and upper stray light regions on the CCD's is changed or switched off, or if the spectral stray light algorithm (or its OPF keydata) is changed, changes will also be observed to the result as shown in figure 2. For additive GDPS algorithms (exposure smear, offset, stray light) this will impact especially the wavelength regions on the CCD detectors where the instrument throughput is low, i.e. the channel overlap regions UV1-UV2 and UV2-VIS.

The swath angle dependence of the irradiance as measured over the on-board quartz volume diffuser is currently calibrated to an accuracy of about 2%, see figure 3. The accuracy of the swath angle dependence of the irradiance will be further improved in the future to below 0.2% for all wavelengths in the full-performance range of the instrument.

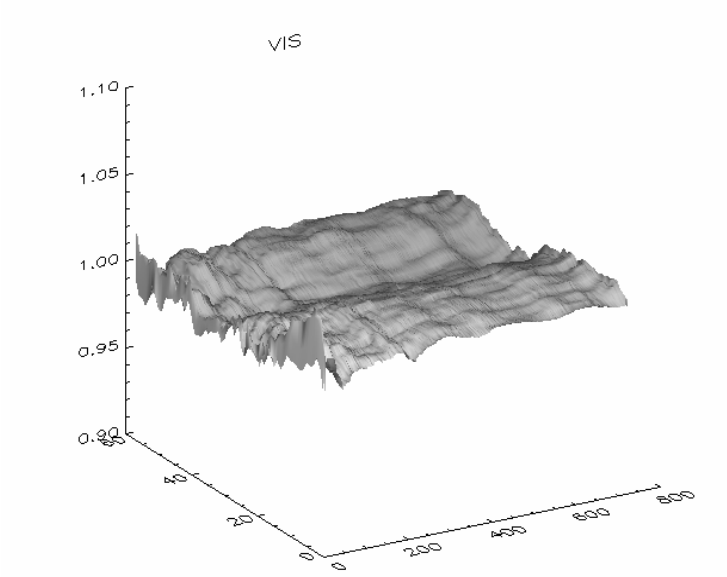


Figure 3: Irradiance swath angle dependence in the VIS channel for orbit 2465 (31 December 2004) for which the azimuth angle is nominal (25.75 degrees). The horizontal axes are the column number (spectral dimension) and row number (viewing angle dimension), the vertical axis is the measured response.

Irradiance-5)
Optical degradation.
During the OMI mission the optical throughput of the instrument will start to degrade at some point. The on-board diffusers and the primary telescope mirror are among the most likely candidates to show evidence of degradation first. Once significant degradation starts to occur it will take some time to describe past degradation and try to predict future degradation accurately and before these characterisation data are fully implemented in the operational data processing chain.
However, at this point in time no significant degradation (i.e. larger than 1%) has been observed in either the earth or the sun mode in the wavelength range 268-504 nm.

Irradiance-6)
Spectral assignment.
The current accuracy of the spectral assignment for both sun and earth spectra is about 0.02 pixel in UV1 and about 0.01 pixel in UV2 and VIS.
A difference of up to 0.01 pixel between the wavelength calibrations from the sun spectra and from the earth spectra has been observed in UV2 and VIS. The reason for this difference is currently not understood.

Irradiance-7)
Besides the spectral stray light algorithm a second stray light algorithm has been implemented in the GDPS, the lower and upper stray light row correction algorithm. This algorithm currently uses the measurement data in the lower and upper stray light areas of the CCD detectors to correct for spatial stray light. First, all column data within the lower row are averaged and the same is done for the upper row. Then the results from the lower and upper areas are averaged and this number is subtracted from all CCD pixels. This is done separately for all subchannels (UV1, UV2, VIS). However, it has been observed that the distribution of the spatial stray light can depend on the row, especially for non-symmetric illumination conditions, like for example close to the south pole or close to the north pole, where only one side of the swath is illuminated. In such cases the lower and upper stray light algorithm will overcorrect areas with lower signal and undercorrect areas

with higher signal. An investigation on stray light is ongoing. Defining updates for the lower and upper stray light area correction algorithm is part of this investigation.
The illumination conditions for the radiance data can be much more inhomogeneous than for the irradiance data, where the illumination is more homogeneous over the viewing angles.

**Level 1 radiance data**

Radiance-1)
Spectral stray light correction.
The spectral stray light correction algorithm that is currently implemented in the 0-1 data processor calculates the source contributions by using measurement data from all viewing directions (rows) and applies the correction to the target region with the same magnitude and wavelength dependence for all rows. This approach was originally chosen to avoid introducing additional measurement noise with the spectral stray light correction algorithm. However, the approach yields incorrect results in case the viewed ground scene is not homogeneous. Viewing directions (rows) with low signals are over-corrected and viewing directions with high signals are under-corrected. The errors can be up to several percent in extreme cases. The error is expected to be least important in UV1, where the spectral stray light correction is most crucial, because the spectral stray light is highest as compared to the useful signal. The reason for this is that the viewed scenes in UV1 are quite homogeneous, because for wavelengths lower than 300 nm the ground and clouds are not observed. Furthermore, the assumption that the stray light distributes more or less homogeneously over all rows in the target region seems to hold rather well for the UV1 subchannel. However, for the UV2 and VIS channels the errors are not negligible. For radiance data the viewed ground scenes are far more inhomogeneous than for the irradiance data.

Radiance-2)
Radiance absolute radiometric calibration.
The radiance absolute radiometric calibration can not be calibrated as straightforwardly as the irradiance, because no accurate comparison standards are readily available. For this reason it was decided to keep for the time being the instrument BSDF as calibrated on the ground as the starting point. This implies that whenever changes are mode to the irradiance, the exact same changes are also made to the radiance in order to ensure that the BSDF is not changed. This includes the swath angle dependence of the (ir)radiance and the instrument BSDF. The absolute central-row BSDF was calibrated accurately (within 1% $1\sigma$) on the ground. The inaccuracies in the swath angle dependence of the BSDF are larger. These inaccuracies transfer also to the swath angle dependence of the earth radiance and reflectance (ratio radiance / irradiance). On the ground the inaccuracies of the BSDF (including swath angle dependence) were considerably larger in the UV1-UV2 and UV2-VIS channel overlap regions as a result of the low instrument throughputs in these wavelength regions.
Given the above the central row absolute radiance is expected to be accurate to within about 2%. The swath angle dependence of the radiance is also expected to be accurate to within about 2%. However, more detailed analyses and comparisons using in-flight data are required to confirm these numbers and improve the accuracies..

Radiance-3)
The geolocation calibration of the radiance level 1 data product is generally accurate to about 3 km. However, from on-ground measurements it is known that the line of sight between in the flight direction can differ between UV1-UV2-VIS by as much as 0.10-0.15 degrees, corresponding to about 1.2-1.8 km at the central nadir position. The UV2 channel looks 'ahead' of the UV1 and VIS channels.

Radiance-4)
Interchannel discontinuities.

In some cases interchannel discontinuities can occur in the earth reflectance data, i.e. the ratio earth radiance over sun irradiance. This originates from the earth radiance data. Figure 4 shows some representative examples.

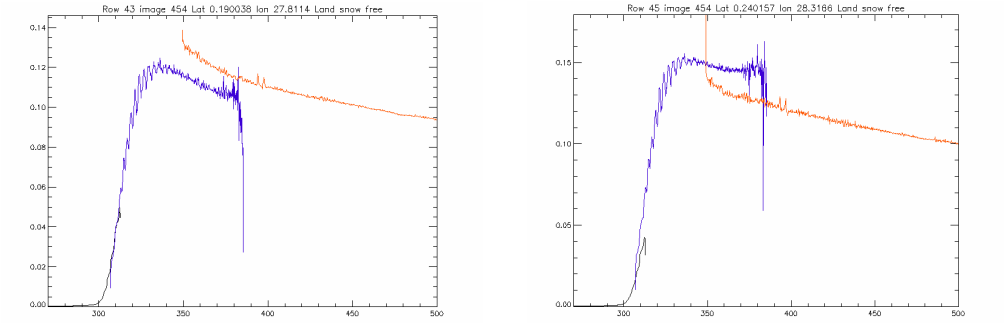


Figure 4: Example of interchannel discontinuities in the reflectance. The left panel shows a negative jump, the UV2 channel lies below the VIS channel. The panel on the right shows a positive jump. The data were taken from orbit 3760, the solar spectrum was taken from orbit 3831.

Further investigation reveals that such interchannel discontinuities are related to pronounced scene changes in the flight direction, for example going from ice to ocean or vice versa, or flying over clouds. However, the correlation between the scene inhomogeneities in the flight direction and the appearance of the interchannel discontinuities in the reflectance is not well-behaved or well-understood. Currently the origin of the discontinuity phenomenon is not understood. It is very likely that the appearance of the discontinuities as exemplified in figure 4 will change when changes are introduced to the various stray light correction algorithms in the GDPS.

Radiance-5)
Optical degradation.
During the OMI mission the optical throughput of the instrument will start to degrade at some point. The on-board diffusers and the primary telescope mirror are among the most likely candidates to show evidence of degradation first. Once significant degradation starts to occur it will take some time to describe past degradation and try to predict future degradation accurately and before these characterisation data are fully implemented in the operational data processing chain.
However, at this point in time no significant degradation (i.e. larger than 1%) has been observed in either the earth or the sun mode in the wavelength range 268-504 nm.
Monitoring the degradation of the primary telescope mirror in the earth mode is difficult, because no known and stable illumination scenes or sources can be used to accomplish this, unlike for example the internal white light source mode or the sun modes. One needs to rely on ground scenes that are sufficiently well understood. Current indications are that the primary telescope mirror has not degraded significantly (i.e. more than 1%).

Radiance-6)
Spectral assignment.
The current accuracy of the spectral assignment for both sun and earth spectra is about 0.02 pixel in UV1 and about 0.01 pixel in UV2 and VIS. For the earth spectra a correction is applied to the wavelength assignment to account for potential scene inhomogeneity (mostly originating from clouds) in UV2 and VIS. This correction can be as large as 0.5 pixel, depending on the scene inhomogeneity (RD06, RD07).
A difference of up to 0.01 pixel between the wavelength calibrations from the sun spectra and from the earth spectra has been observed in UV2 and VIS. The reason for this difference is currently not understood.

Radiance-7)

Besides the spectral stray light algorithm a second stray light algorithm has been implemented in the GDPS, the lower and upper stray light row correction algorithm. This algorithm currently uses the measurement data in the lower and upper stray light areas of the CCD detectors to correct for spatial stray light. First, all column data within the lower row are averaged and the same is done for the upper row. Then the results from the lower and upper areas are averaged and this number is subtracted from all CCD pixels. This is done separately for all subchannels (UV1, UV2, VIS). However, it has been observed that the distribution of the spatial stray light can depend on the row, especially for non-symmetric illumination conditions, like for example close to the south pole or close to the north pole, where only one side of the swath is illuminated. In such cases the lower and upper stray light algorithm will overcorrect areas with lower signal and undercorrect areas with higher signal. An investigation on stray light is ongoing. Defining updates for the lower and upper stray light area correction algorithm is part of this investigation.
The illumination conditions for the radiance data can be much more inhomogeneous than for the irradiance data, where the illumination is more homogeneous over the viewing angles.

**Earth reflectance data**

The individual radiance and irradiance data products may contain a number of artefacts that are residuals of corrections in the 0-1 data processing that are not perfect. In many cases (e.g. PRNU, slit irregularity) such corrections are exactly the same for the radiance and the irradiance data products and when the ratio of radiance over irradiance (called the earth reflectance) is calculated potential non-optimal corrections cancel. This implies that the derived earth reflectance data product is in many aspects more accurate than the individual radiance or irradiance data products. Evaluations and comparisons on the reflectance data have shown that the absolute earth reflectance for the nadir viewing direction is currently accurate to about 2%. The swath angle dependence of the reflectance appears to be accurate also to within 2%. More detailed analyses and comparisons using in-flight data are required to confirm these numbers and to improve the accuracies.
Note that the earth reflectance data is not an official output data product of the 0-1 data processor. The earth reflectance data can be calculated by the data user from the radiance and irradiance data products.